Cytotoxicity of a Vanadyl(IV) Complex with a Multidentate Oxygen Donor in Osteoblast Cell Lines in Culture

J. Rivadeneira[1,2], A.L. Di Virgilio[1], D.A. Barrio[1], C.I. Muglia[1], L. Bruzzone[3] and S.B. Etcheverry[1,2,*]

[1]*Cátedra de Bioquímica Patológica, Facultad de Ciencias Exactas, Universidad Nacional de La Plata, 47 y 115 (1900) La Plata, Argentina;* [2]*Centro de Química Inorgánica (CEQUINOR_CONICET), Facultad de Ciencias Exactas, Universidad Nacional de La Plata, 47 y 115 (1900) La Plata, Argentina;* [3]*División Química Analítica, Facultad de Ciencias Exactas, Universidad Nacional de La Plata, 47 y 115 (1900) La Plata, Argentina*

Abstract: Strong chelating ligands as oxodiacetate (oda) are model systems to study the process of metal trapping by living organisms. Vanadium compounds display interesting biological and pharmacological actions. In vertebrates, vanadium is stored mainly in bones. In the present study we report the effects of the complex of oda with vanadyl(IV) cation, VO(oda), on two osteoblast cell lines, one normal (MC3T3E1) and the other tumoral (UMR106). VO(oda) exerted cytotoxic actions in osteoblasts as it was determined through a dose-dependent decrease in cell proliferation, and morphological and actin alterations. The putative mechanisms underlying VO(oda) deleterious effects were also investigated. The complex increased the level of ROS which correlated with a decreased in GSH/GSSG ratio. Besides, VO(oda) induced a dissipation of the mitochondria membrane potential (MMP) and promoted an increase in ERK cascade phosphorylation, which is involved in the regulation of cellular death and survival. All the effects were more pronounced in MC3T3-E1 than in UMR106 cells. ERK activation was inhibited by PD98059, Wortmanin and the ROS scavenger NAC (N-acetyl cysteine). These results suggest that VO(oda) stimulated ERKs phosphorilation by induction of free radicals involving kinases upstream of ERK pathway. The inhibitory effect of the complex on cell proliferation was partially reversed in both cell lines by NAC. Moreover, PD98059 and Wortmanin also partially reversed the inhibition of cell proliferation in the tumoral osteoblasts. The use of specific inhibitors and ROS scavengers suggested the involvement of oxidative stress, MMP alterations and ERK pathway in the apoptotic actions of this complex.

Keywords: Vanadium cytotoxicity- chelating ligands-osteoblasts- cellular morphology- oxidative stress-mitochondria membrane potential-GSH/GSSG ratio- ERK phopsphorylation

1. INTRODUCTION

Strong chelating ligands are very important in aqueous media because they offer the opportunity of trapping different metal species [1]. This process becomes particularly significant in living systems, where different metals are acquired, transported and stored mostly by low-molecular-weight compounds involving multidentate oxygen donors from carboxylate, hydroxamate and catecholate ligands [2, 3].

Among the family of multidentate oxygen donor species, oda= oxodiacetate, $O(CH_2COO^-)_2$, stands as a versatile complexing agent, having the potential O-donor atoms in different orientations, thus allowing the construction of networks of different dimensionalities. As a ligand, oda holds an OOO donor set and can complex metal ions by forming chelate rings. As an example, a new polymeric phase of zinc(II) oxodiacetate has been reported [4].

This ligand has been extensively used showing the ability of oxodiacetate to form polymeric species via bridging modes, and several structures containing this anion in different environments [5].

*Address correspondence to this author at the Bioquímica Patológica, Facultad de Ciencias Exactas, UNLP, 47 y 115 (1900) La Plata, Argentina; Tel: +54 221 423 5333 ext 49; Fax: +54 221 4259485;
E-mail: etcheverry@biol.unlp.edu.ar

On the other hand, vanadium is a transition element broadly distributed in nature in trace amounts [6, 7]. Concerning animals and human beings, vanadium compounds, once absorbed, are retained mainly in bones [6, 8]. Although the essentiality of vanadium for man is still unknown it has been reported that vanadium derivatives are potentially useful drugs from a pharmacological point of view. In fact, vanadium compounds have been shown to display potential therapeutic applications as insulin mimics, [9, 10] antineoplastic drugs [11-13] and more recently some osteogenic effects have also been reported [14-16]. In particular, we are very interested in the antitumoral actions of alternative potential compounds such as vanadium derivatives to provide a broad source of compounds worthy to be tested for cancer treatments in a near future. Some vanadium compounds have shown deleterious effects on tumoral cell proliferation and differentiation as well as on cellular morphology [17-20]. This antitumoral action seems to be mediated through different mechanisms. Among these pathways, the induction of phosphorylation of tyrosine residues seems to play a major role. This effect may be due to the inhibition of key protein tyrosin phosphatases (PTPases), which in turn promotes the activation of the extracellular regulated kinase (ERK) pathway [21-24]. Besides, changes in cell cytoskeleton proteins [20, 25] as well as an increment in the oxidative stress (production of reactive oxygen species (ROS) [26-28], alterations in the ratio GSH/ GSSG [29, 30] induction of apoptosis

1573-4064/10 $55.00+.00

[9, 17, 31] and diverse direct and indirect effects on DNA synthesis and breakdown have also been described as putative mechanisms of action [32-34]. It has been reported that vanadium can also cause toxic actions in living systems [35-38]. To understand the toxicity of vanadium compounds it is essential to know the mechanisms of action as well as the susceptibility of different cells.

Del Río and col. have previously reported the synthesis of the complex bis(aqua)oxodiacetatooxovanadium(IV) of vanadyl cation with the ligand oda, VO(oda) (Fig. **1**). [39]. Besides, the spectroscopic characterization of this complex and its bioactivity in osteoblast-like cells in culture have been recently determined [40]. Although VO(oda) was previously reported as an antiapoptotic compound in RINm5F cells that produce insulin, [41] the complex displayed deleterious effects in osteoblasts in culture since it caused inhibition of cell proliferation and differentiation in a normal and in a tumoral osteoblast cell lines.

The aim of the present study is to extend our previous observations on the bioactivity of VO(oda) in osteoblasts, focusing the attention on its cytotoxic effects trying to elucidate its mechanisms of action.

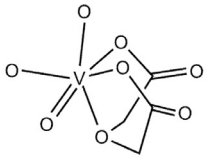

Fig. (1). Schematic structure of the complex bis(aqua)oxodiacetatooxovanadium(IV) (VO(oda)).(Adapted from reference [39]).

2. RESULTS

2.1. VO(oda) Induces Cytotoxicity in Osteoblasts in Culture

Our research group has recently reported the effect of the complex on the proliferation of two osteoblast cell lines: MC3T3-E1 derived from mouse calvaria and UMR106 derived from a rat osteosarcoma. [40] VO(oda) significantly inhibited osteoblast growth in a dose dependent manner after 24 h of incubation but with different responses in both cell lines ($p<0.001$).

Besides, we have also shown that the complex significantly inhibited the alkaline phosphatase activity, a marker of osteoblast differentiation, in the UMR106 osteoblast-like cells. [40]

To quantify the deleterious effect of the complex we have now determined the IC_{50} in both cell lines. A stronger response was observed in MC3T3-E1 cells (IC_{50}= 50 μM) than in UMR106 tumoral osteoblasts (IC_{50} >100 μM). It can be seen that the complex caused greater cytotoxicity in the non-transformed osteoblasts than on the tumoral ones.

2.1.1. Effects of VO(oda) on Lysosomal Activity. Neutral Red Assay

The metabolically active lysosomes display the capacity of uptake the neutral red dye (NR). The cytotoxic effects of VO(oda) on the non- transformed osteoblast cell line MC3T3-E1 affects the functions of lysosomes. This effect can be observed in Fig. (**2**).

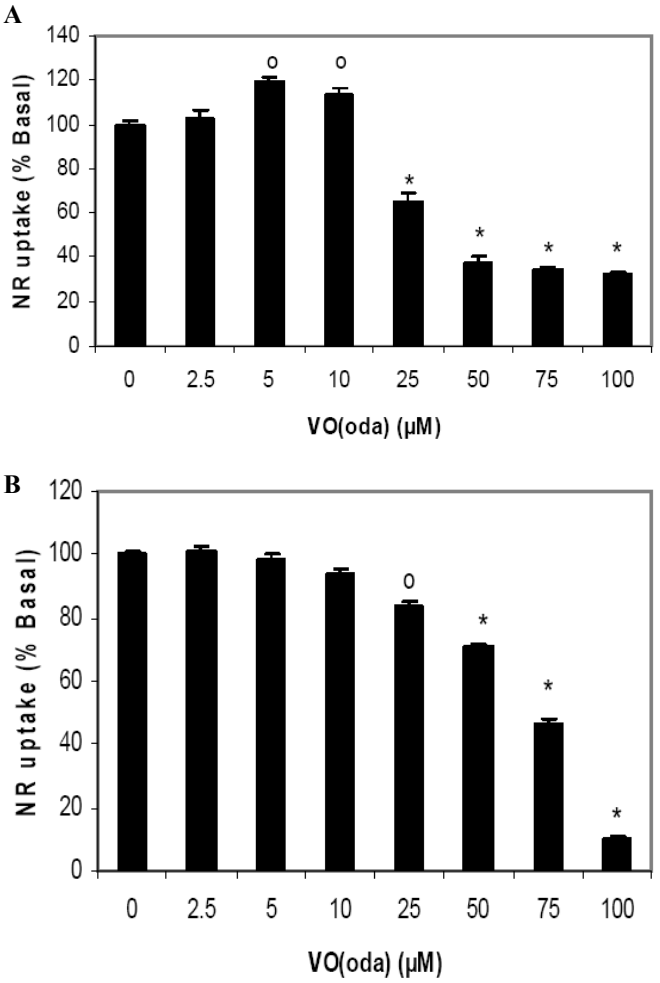

Fig. (2). Neutral red uptake by osteblasts in culture. MC3T3-E1 osteoblast-like cells (A) and UMR106 osteosarcoma derived osteoblasts (B) were incubated with different doses of VO(oda) for 24 h at 37 ° C. After incubation, cell viability was determined by the uptake of neutral red. The dye taken up by the cells was extracted and the absorbance read at 540 nm. Results are expressed as % basal and represent the mean ± SEM, n=16, ºp<0.05; *p<0.001.

As can be seen the lowest tested concentration (2.5 μM) did not show any difference with the control condition (without complex addition). Nevertheless, at 5 and 10 μM a statistically significant increase in the uptake of the dye by the lysosomes of the osteoblasts could be detected. As the concentrations of VO(oda) increase, a marked cytotoxic effect could be observed in the 25-100 μM range.

On the other hand, in the tumoral cell line UMR106, a decrease of the lysosomal activity was detected from 25 μM with a marked decrease at 100 μM. These results agree quite well with the effects of the complex on the proliferation of tumoral osteoblasts [**Error! Bookmark not defined.**] since the deleterious effects of the complex on the UMR106 cell proliferation could be seen from 25 μM.

The alteration on the lysosomal activity may be one of the factors that play a role on the VO(oda) cytotoxicity.

2.2. Morphological Changes

To further investigate the cytotoxicity of VO(oda) in osteoblasts in culture, we next determined the effect of this complex on the morphology of MC3T3-E1 and UMR106 cells. As can be seen from Fig. (**3A**), the MC3T3-E1 control monolayers showed the aspect of a typical fibroblast-like culture. Cells are arranged in a star-like manner and present round nuclei. Many processes connect each cell with their neighboring. The deleterious effect of VO(oda) could be observed at 10 μM concentration (Fig. **3B**). A gradual cytoplasm condensation and loss of the connections between the cells could be observed as the concentrations of the complex increase. At 100 μM concentration, the most pronounced changes were observed; the nuclei were pyknotic; besides, scarce and very thin cytoplasmic connections between cells can be observed. In addition, an important number of cells died and detached from the monolayers (Fig. **3C**).

The morphological characteristics of a culture of UMR106 osteosarcoma cells can be seen in Fig. (**3D**). These cells showed polygonal shape and nuclei of irregular forms. Cells connected with their neighbors through lamellar processes. Nuclear and cytoplasm condensation were observed after the incubation with VO(oda) 10 μM (Fig. **3E**). The number of processes between the cells diminished as well as the number of cells per field. Besides, nuclear pyknosis with chromatine condensation and apoptotic bodies were observed (see arrow). The limits of the cells were undefined and difficult to observe. The cells exhibited dense nuclei surrounded by very little and highly condense cytoplasm at 100 μM (Fig. **3F**).

Altogether, both cell lines displayed features typical of apoptosis after the treatment with the complex.

2.3. Alterations in Cytoskeleton Actin

The described morphological alterations are based on the modifications of the cytoskeleton proteins. The cytoskeleton network can be observed by the staining of the actin fibers with Phalloidin-FITC, a fluorescent probe with high affinity for the cytoskeleton. Fig. (**4**) (upper panel) shows the organization of actin filaments in MC3T3-E1 cells. The characteristics of actin architecture are depicted in Fig. (**4A**) (control cells) and in (Figs. **4B** and **4C**) for the osteoblasts treated with growing doses of the complex (10 μM and 100 μM, respectively). Under normal conditions (without complex addition), the osteoblasts present actin microfilaments placed in the direction of the main axis of the cells. In the presence of the vanadium complex, a rearrangement of the actin network is observed as well as important alterations in the shape of the cells. At 100 μM, the cells showed the actin accumulated in some cytoplasm ‘‘patches’’.

The pictures in Fig. (**4**) (lower panel) show the characteristics of the actin filaments in UMR106 cells. Control tumoral cells (Fig. **4D**) displayed a pattern similar to that of control MC3T3-E1 cells. When the osteosarcoma cells were treated with different concentrations of VO(oda) the regularity of this pattern becomes alter as the concentrations of the drug increased. For these tumoral cells the first changes in actin microfilaments organization could be seen at 25 μM (Fig. **4E**). At 100 μM, a complete disorganization was visualized with the fibers surrounding the nuclei of the cells and

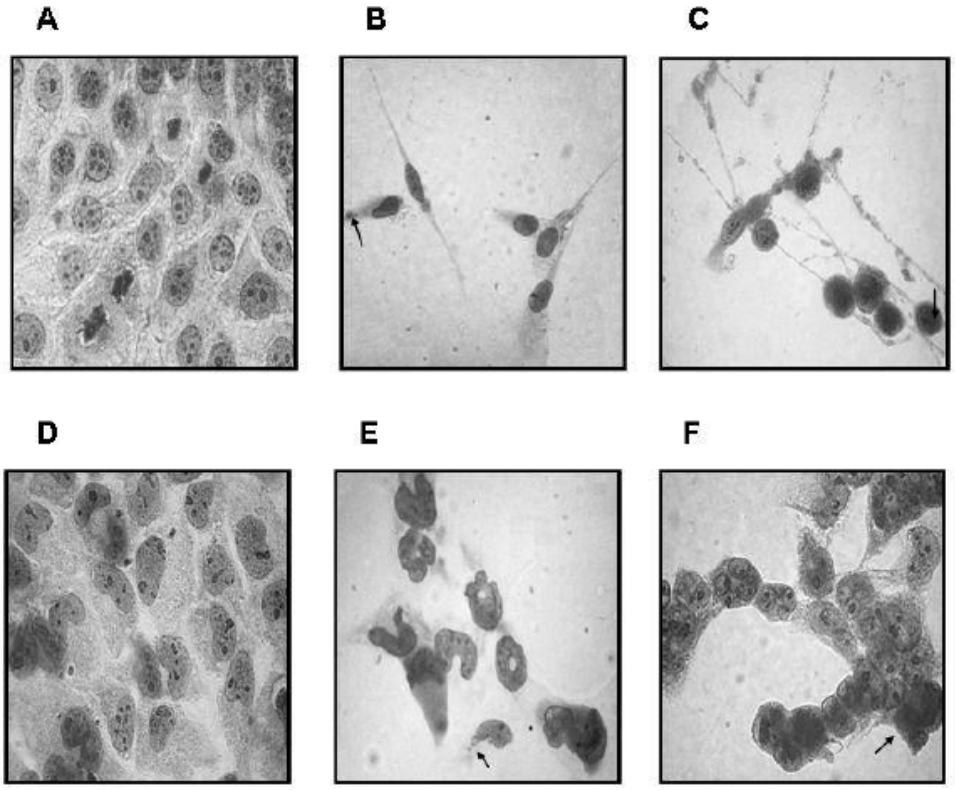

Fig. (3). Effect of VO(oda) on osteoblast morphology: MC3T3-E1 cells (upper panel) and UMR106 cells (lower panel). Cells were incubated with VO(oda) for 24 h. Then, the cells were stained with Giemsa and observed by light microscopy (Magnification 100 X).

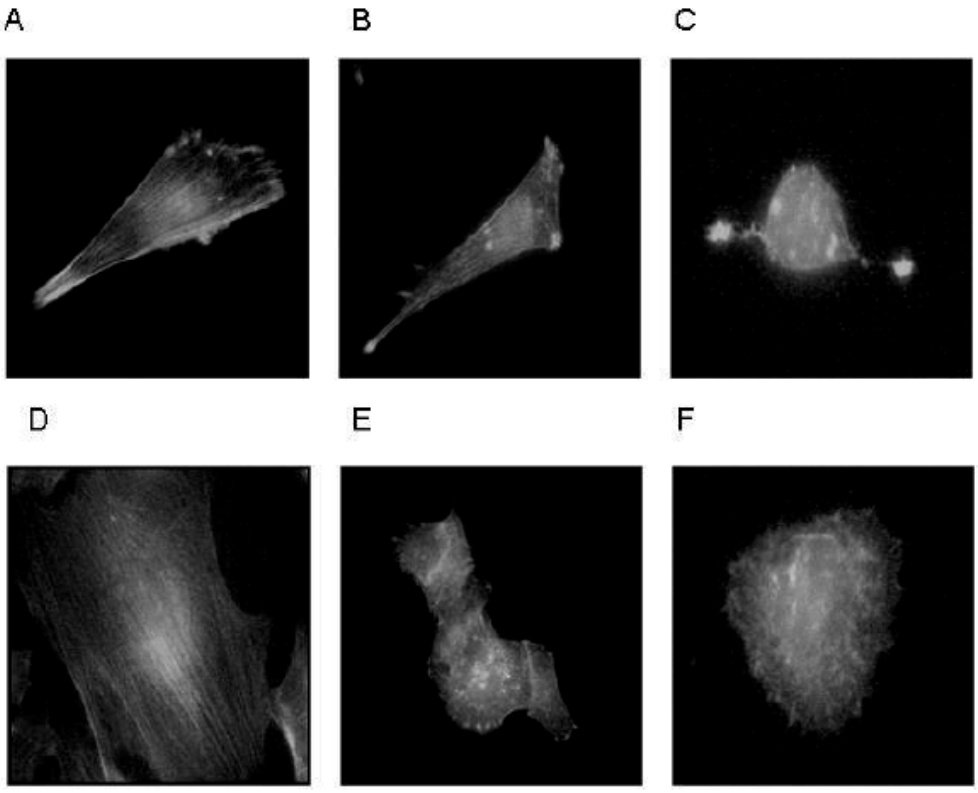

Fig. (4). Effect of VO(oda) on the actin cytoskeleton filaments of MC3T3-E1 (Fig. A,B,C) and UMR106 cells (Fig. D,E,F), see text. Cells were incubated with different concentrations of VO(oda) for 24 h at 37 ºC. Then, the cells were stained with Phalloidin-FITC and observed by fluorescence microscopy (Magnification 100X).

the shape of cells completely altered (Fig. **4F**). The intensity of the observed changes was stronger in the non-transformed osteoblasts than in the tumoral cells. This result is in accordance with the morphological and the proliferation studies.

2.4. Reversibility Study

In order to establish if the deleterious effect of VO(oda) was reversible, the cells were incubated with increasing concentrations of the complex for 24 h at 37 ºC. After this period, the culture was washed to eliminate the complex. Then, Dulbecco's Modified Eagle's Medium (DMEM) plus 10% fetal bovine serum (FBS) was added and the osteoblasts were cultured for another 24 h under this condition. The results can be seen in Fig. (**5**). After 24 h of incubation with VO(oda) it could be observed a decrease in cell proliferation that was significant from 25 μM compared with control for both cell lines. Nevertheless, a great number of cells that survived alter this 24 h incubation with the complex, lost their ability to proliferate under optimal culture conditions for another 24 h in the absence of VO(oda). This effect can be seen in the lower curves of (Fig. **5**), since the number of cells under this condition was significantly lower than that of the first period of 24 h incubation (upper curve in Fig. **5**). Besides, it can be seen from (Fig. **5**) that differences statistically significant between both culture conditions begun at 25 μM for MC3T3-E1 cells and at 50 μM for UMR106 tumoral cells. The damage caused by the complex did not revert and on the contrary, it turned worse indicating that the alterations were irreversible.

2.5. Evaluation of Putative Cell Death Mechanisms

The possible mechanisms of cell death triggered by VO(oda) were investigated through the determination of the oxidative stress (ROS production) and the evaluation of the redox couple GSH/GSSG. Besides, the effect of the complex on the alteration of the mitochondria membrane potential (MMP) and the activation of ERKs pathway were also investigated.

2.5.1. Determination of Reactive Oxygen Species. Intracellular ROS Production

This assay was carried out using DHR-123 that is a not fluorescent compound. This probe determines the levels of intermediate peroxynitrite, hydroxyl radicals and hydrogen peroxide [42-44].

In the cells, DHR-123 was oxidized to Rhodamine123 in the presence of oxidizing drugs. Because fluorescent oxidation products are only produced in metabolically active cells, DHR-123 can also be used as a viability indicator. Cell extracts for rhodamine measurements were obtained and processed as previously described, using fluorescence spectroscopy [45]. As can be seen from (Fig. **6**), VO(oda) induced a dose-dependent oxidative stress in both cell lines with a stronger response in the non- transformed osteoblasts. Significant differences *vs*. basal could be observed from 10 μM for MC3T3-E1 cells and from 50 μM for the UMR106 tumoral osteoblasts ($p<0.001$). These results suggest that the damage caused by oxidative stress is more pronounced in the non-transformed osteoblasts.

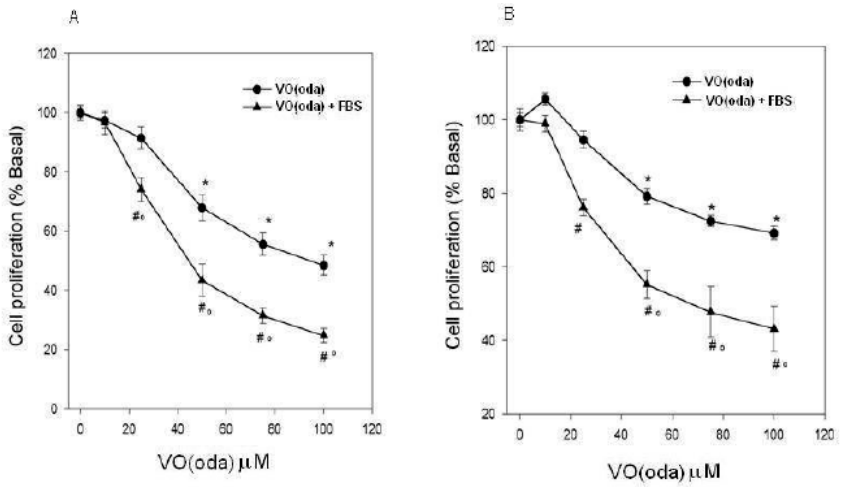

Fig. (5). Reversibility of cytotoxic effect induced by VO(oda) in MC3T3-E1 (A) and UMR106 cells (B). Osteoblasts were incubated with different concentrations of VO(oda) for 24 h at 37ºC and cell proliferation determined by the crystal violet assay (upper curves). Then, the conditioned medium was eliminated and the potential recovery of cell viability was determined in DMEM plus 10% FBS, without complex addition, at 37 °C for 24 h (lower curves). Results are expressed as the mean ± SEM, n=6, *, # significant differences vs. control, º values significantly different comparing both treatments.

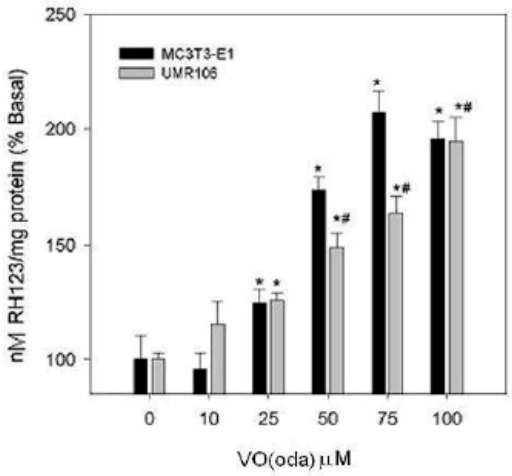

Fig. (6). Induction of ROS by VO(oda) in MC3T3-E1 and UMR106 cells. Cells were incubated with growing concentrations of VO(oda) at 37 °C for 24 h . ROS production in the cells was evaluated through the oxidation of DHR-123 to Rhodamine123. Results represent the mean ± SEM, n=6, *significant differences vs. control, # significant differences between the two cell lines.

On the other hand, the determination of ROS level in MC3T3-E1 cells in the presence of 0.1 mM of the antioxidant drug N-acetyl cysteine (NAC), can be seen in Fig. (**7A**). NAC produced a partial reversion on the oxidative stress induced by VO(oda) with statistically significant differences for the higher concentrations. Similar effect could be seen in the tumoral cell line (Fig. **7B**), but using a higher concentration of NAC (0.25 mM).

The reported results indicate the relevance of the oxidative stress as a major factor of the cytotoxic effects caused by VO(oda). To verify this assumption, the proliferation assay was carried out in the presence of VO(oda) and NAC. As can be seen from (Fig. **8A**), the decrease in cell proliferation was partially reversed by the addition of 100 μM NAC to the culture dishes of MC3T3-E1 cells. In the case of the tumoral osteoblasts similar results were obtained with 250 μM NAC (Fig. **8B**).

2.5.2. Determination of the Ratio GSH/GSSG

Reduced glutathione (GSH), with a free thiol group, is a major antioxidant in mammalian tissues that is involved in numerous metabolic pathways. It provides reducing equivalents for the glutathione peroxidase catalyzed reduction of hydrogen peroxide and lipid hydroperoxides to water and the respective alcohol. During this process GSH is oxidized to GSSG. The GSSG is then recycled into GSH by glutathione reductase.

When mammalian cells were exposed to increased oxidative stress, the ratio GSH/GSSG decreased as a consequence of GSSG accumulation. Measurement of the GSSG level or determination of the GSH/GSSG ratio is another useful indicator of oxidative stress.

Fig. (**9**) shows the effect of different doses of the complex on the ratio GSH/GSSG in both cell lines. As can be observed this ratio decayed for 50 and 100 μM in both cell lines. Otherwise, at 100 μM, the decrease of the ratio was greater for the non-transformed osteoblasts than for the osteosarcoma cells. Besides, Fig. (**10**) shows the GSH concentration level in both osteoblastic lines. The results indicated that in the UMR106 cells, the level of GSH was about twice the level of the non-transformed osteoblasts (6.15 ± 0.39 μg GSH/mg protein *vs*. 3.47 ± 0.26 μg GSH/ mg protein, respectively). In both cell lines, the GSH level decreased at 50 and 100 μM.

On the other hand, an acute stress caused by the addition of 200 μM VO(oda) for a short period to osteoblast cultures produced a marked decrease in the GSH/GSSG ratio. This effect was more pronounced in the tumoral cells although these cells manage to recover earlier (4 h culture) than the normal osteoblasts (Fig. **11**). This fact may be related to the approximately double concentration of GSH in the basal

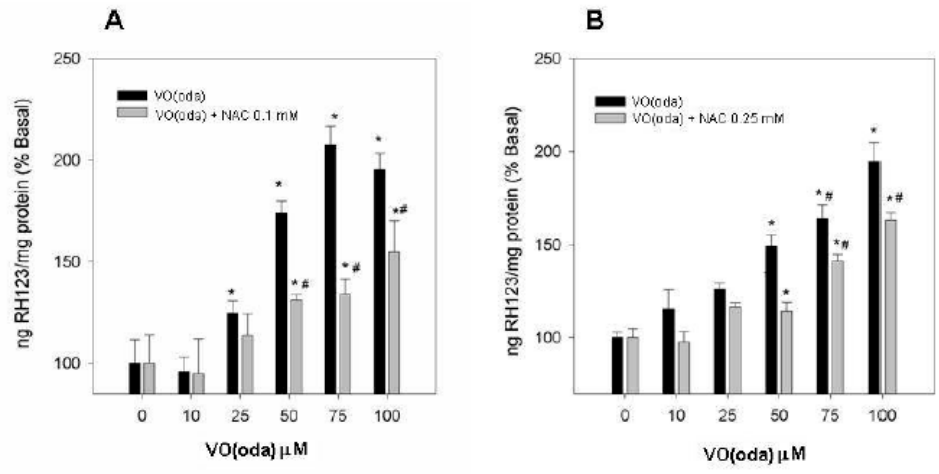

Fig. (7). Effect of VO(oda) on ROS production in the presence of NAC in MC3T3-E1 osteoblasts (A) and UMR106 cells (B). Cells were incubated with different concentrations of VO(oda) or VO(oda) plus NAC 0.1 mM for MC3T3-E1 and 0.25 mM for UMR106 during 24 h. Results are expressed as mean ± SEM, n=6. For both cell lines: * significant differences vs. control, # significant differences in relation to the same dose of the complex in absence of NAC.

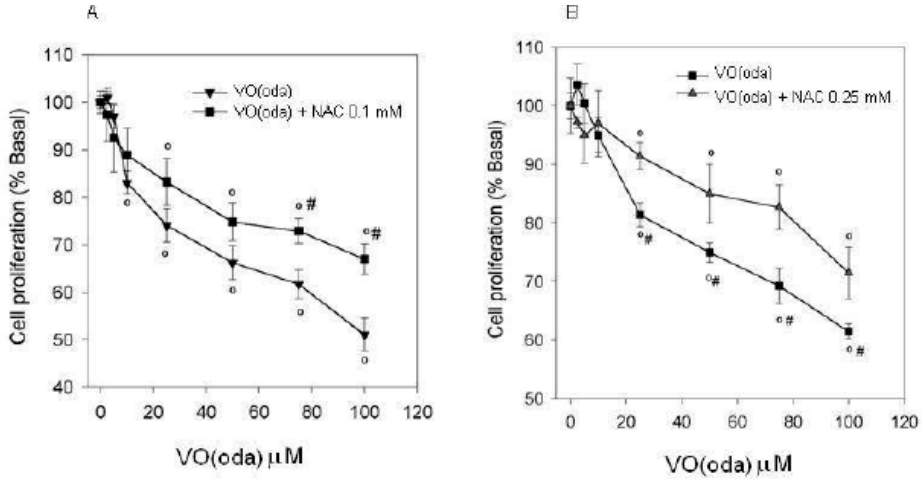

Fig. (8). Effect of VO(oda) on cell proliferation in presence of NAC in MC3T3-E1 (A) and UMR106 cells (B). Cells were incubated with different VO(oda) concentrations or VO(oda) plus 100 μM NAC for MC3T3-E1 and 200 μM for UMR106 cells during 24 h. Results are expressed as mean ± SEM, n=6. For both cell lines: º significant differences vs. control, # signicant differences between treatments.

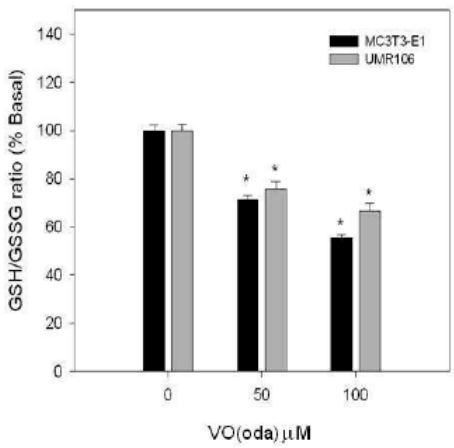

Fig. (9). GSH/GSSG ratio in MC3T3-E1 (A) and UMR106 cells (B), incubated with different concentrations of VO(oda). Results are expressed as mean ± SEM of three independent experiments, * significant differences vs. basal.

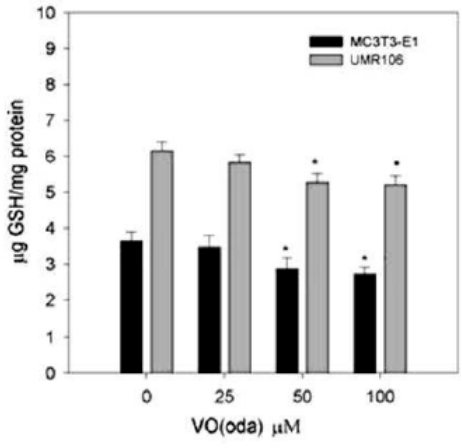

Fig. (10). GSH level in MC3T3-E1 and UMR106 osteoblast-like cells in presence of different VO(oda) concentrations. Results expressed the mean ± SEM of three independent experiments, * significant differences vs. basal.

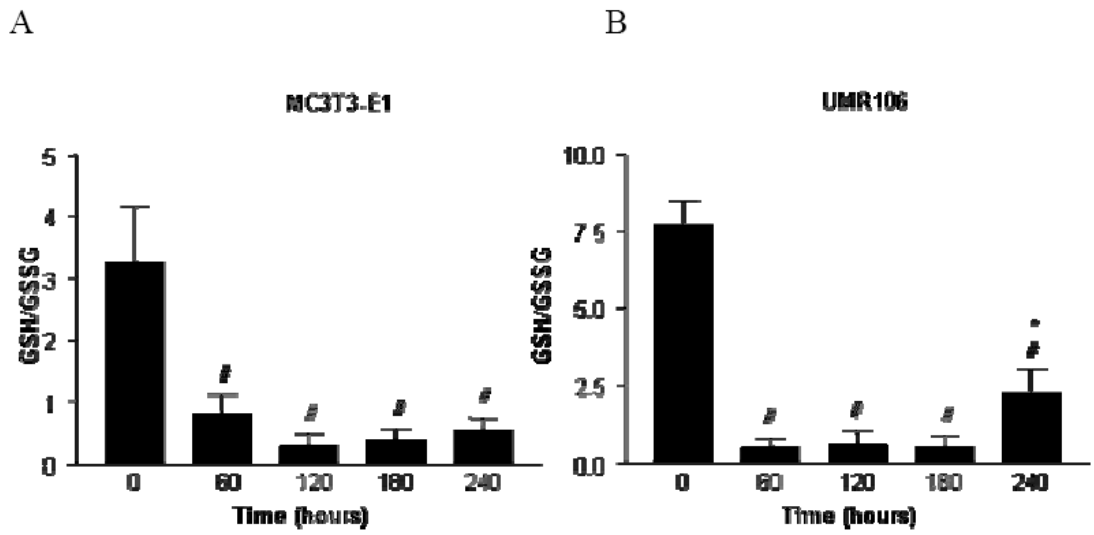

Fig. (11). Time course of the effect of VO(oda) on GSH/GSSG ratio in osteoblasts in culture. Confluent MC3T3-E1 (A) and UMR106 (B) cells were incubated with 200 μM VO(oda) during different periods of time (0-4 h). Results are expressed as GSH/GSSG ratio and represent the mean ± SEM, of three independent experiments carried out by triplicate, ≠ significant differences vs basal, $p<0.001$, * indicate the recovery of GSH/GSSG ratio in the tumoral cells at 4 h after treatment.

condition of the UMR106 cells compared with MC3T3-E1 osteoblasts.

On the other hand, to analyze the influence of the cellular redox status on VO(oda) cytotoxicity, we carried out a new proliferation assay incubating MC3T3-E1 cells with different concentrations of VO(oda) plus 3 mM GSH (Fig. **12**). A complete reversion of the deleterious action of the complex could be observed. Similar results were obtained for the UMR106 cells with 1 mM GSH.

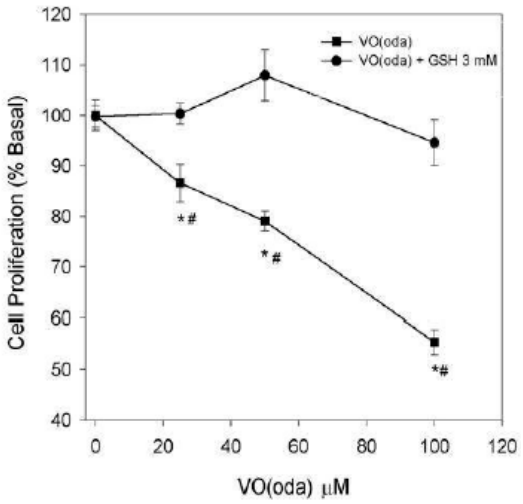

Fig. (12). Effect of VO(oda) on MC3T3-E1 cell viability in presence of GSH. Cells were incubated during 2 h with 3 mM GSH and then, different concentrations of the complex were added at 37 ºC for 24 h. Results are expressed as the mean ± SEM, n=9, * significant differences vs. control, # significant differences between treatments.

To confirm that the depletion of GSH was one of the mechanisms involved in the cytotoxicity of VO(oda), additional cultures were performed with VO(oda) plus L-Buthionine sulfoximide (BSO), an inhibitor of GSH synthesis. Under these conditions, MC3T3-E1 cells showed more pronounced toxic effects than when they were incubated only in the presence of the complex, establishing the crucial role of GSH level in the survival of the osteoblasts (Fig. **13**). Similar results were obtained for the tumoral cells.

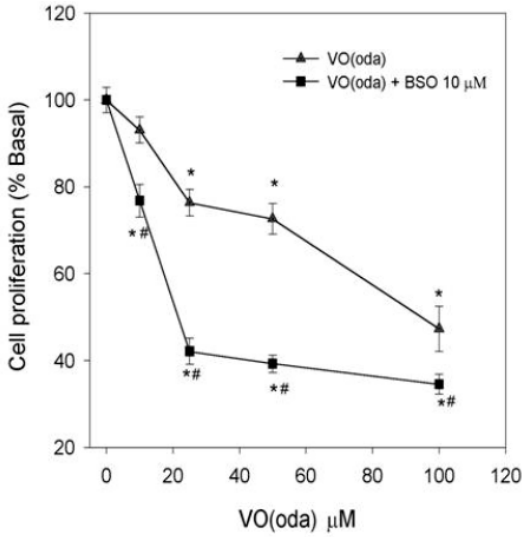

Fig. (13). Effect of GSH depletion on cell viability in presence of VO(oda) in MC3T3-E1 cells. Osteoblasts were incubated with 10 μM BSO overnight. After that, growing concentrations of VO(oda) were added and the cells were incubated at 37 ° C for 24 h. Results represent the mean ± SEM, n=9, *significant differences *vs*. control, # significant differences between treatments.

Altogether, these results suggest that the UMR106 cells are more protected against the oxidative stress than the non transformed osteoblasts, in agreement with the levels of ROS

measured by the DHR-rhodamine 123 assay discussed above.

2.5.3. Alterations of the Mitochondria Membrane Potencial (MMP)

To elucidate if VO(oda) induced cytotoxicity in osteoblasts by alterations of mitochondria functions, we evaluated the MMP in both cell lines under control conditions and in the presence of VO(oda). Moreover, due to the fact that a decline in the MMP usually occurs along with an alteration in the cellular redox status, the relationship between MMP and oxidative stress was investigated in the presence of GSH. MC3T3-E1 cells were incubated with 50 and 100 µM VO(oda), and with 100 µM VO(oda) plus 3 mM GSH for 24 h. The changes in MMP were measured by flow cytometry using the probe Rodamine 123. Fig. (**14A**) showed the results for MC3T3-E1 cells. As can be seen, the fluorescence intensity of Rodamine 123 shifted to the left, indicating the dissipation of MMP as the dose of the complex increased. The fractions of cells that displayed low fluorescence intensity were 7, 35 and 41% for 0, 50 and 100 µM VO(oda), respectively. The last picture of this figure shows that the addition of 3 mM GSH maintained the MMP at control level confirming again that the VO(oda) cytotoxicity was mediated by the oxidative stress and that the GSH level played a major role in the cell survival. Besides, these results indicated that the MMP dissipation is a down stream event of the ROS generation.

Fig. (**14B**) shows the results obtained in UMR106 osteosarcoma cells. In the tumoral osteoblasts, it could also be observed a dose dependent loss of MMP. Nevertheless, in this case, the fractions of cells with low fluorescence intensity were lower than those determined for MC3T3-E1 cells at similar doses of the complex: 5%, 20% and 27% at 0, 50 and 100 µM, respectively. Moreover, pre-incubation of the tumoral osteoblasts with 1 mM GSH prevented the loss of MMP induced by the complex.

As a whole, these results are in agreement with those obtained by the crystal violet assay, DHR-123 oxidation test and the variation in the ratio GSH/GSSG.

2.5.4. VO(oda) Induced the Activation of ERK-1/2 in Osteoblast-Like Cells

The cascades of the protein kinases activated by mitogens (MAPK) and the phosphatidyl inositol-3 kinase (PI3-K) are involved in the regulation of cellular death and survival. The activation of ERK cascade by VO(oda) was evaluated using a method previously described [46]. Proteins in the cell extracts were separated by SDS-PAGE and examined by immunoblotting with specific antibodies against the phosphorylated and non-phosphorylated forms of ERK-1/2. Representative immunoblots of the effect of the complex on UMR106 cells is shown in Fig. (**15**).

The complex stimulated ERK phosphorylation in a dose dependent manner from 100 to 1000 µM. Relative intensities of stimulation of the ERK cascade were corrected for total ERK as determined by densitometry and were expressed as % basal as can be seen in the lower part of the Fig. (**15**). In the UMR106 cell line, the relative intensities of PERK reached a maximum of 275 at 1000 µM while in the non-transformed osteoblasts this maximum was about 430 (data not shown). These results indicate that the ERK pathway may be involved in the VO(oda) cytotoxic effects.

In an attempt to define the mechanism by which VO(oda) induced ERK phosphorylation, the potential role of the oxi-

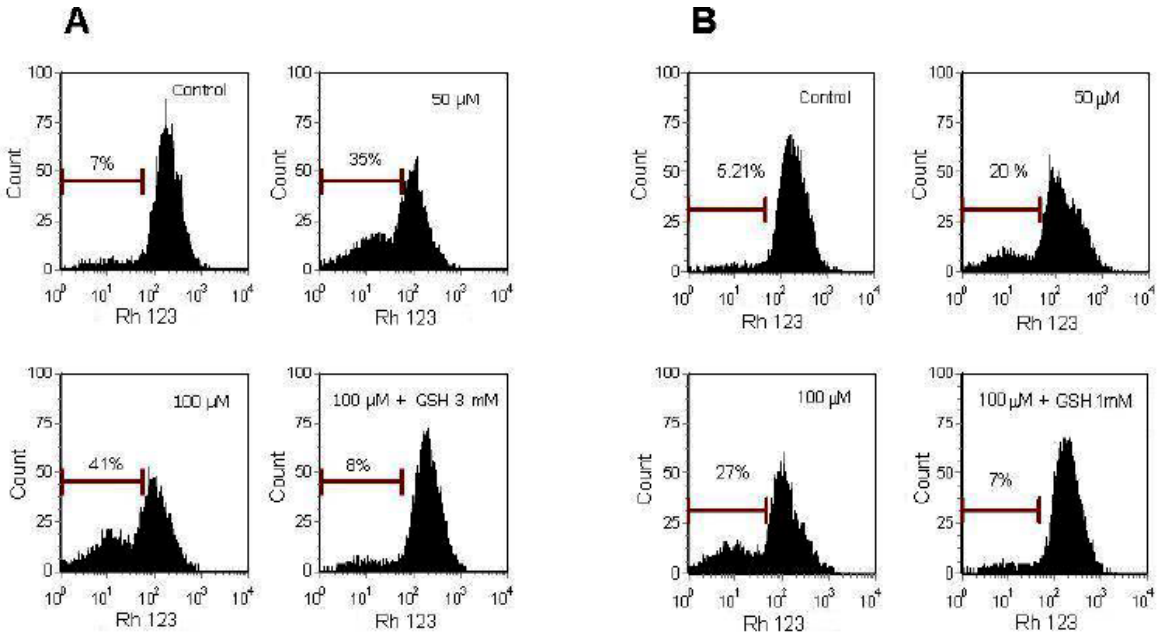

Fig. (14). Effect of VO(oda) on the mitochondria membrane potential (MMP) in MC3T3-E1 osteoblast-like cells **(A)** and UMR106 osteosarcoma cells **(B)**. Osteoblasts were incubated with 50 and 100 µM VO(oda), or with 100 µM VO(oda) plus 3 mM GSH for MC3T3-E1 cells and 1 mM GSH for UMR106 cells, at 37 ºC for 24 h. Results were obtained using flow cytometry and each histogram is representative of three independent experiments.

dative stress and MAPK pathway was evaluated using specific inhibitors: wortmanin (a PI3-K inhibitor), PD98059 (a MEK inhibitor) and NAC (a free radical scavenger) (Fig. **16**). The activation of ERK-1/2 was inhibited by PD98059, wortmanin and NAC. These results suggest that VO(oda) stimulated ERK phosphorylation by induction of ROS or the activation of PI3-K and MEK pathways.

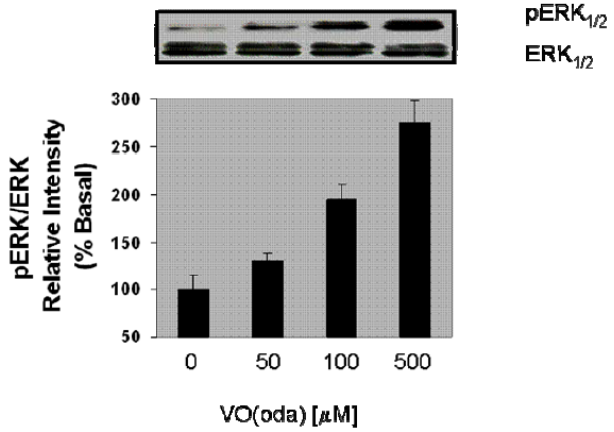

Fig. (15). Dose-response of VO(oda)-induced ERK-1/2 phosphorylation. Confluent UMR106 cells were treated with different concentrations of VO(oda) for 1 h. Cells were lysated in Laemmli buffer and analyzed by Western Blot. Relative intensities of stimulation were corrected for total ERK, as determined by densitometry. Results are expressed as % basal and represent the mean ± SEM of three independent experiments, *significant difference vs. basal, $p<0.001$.

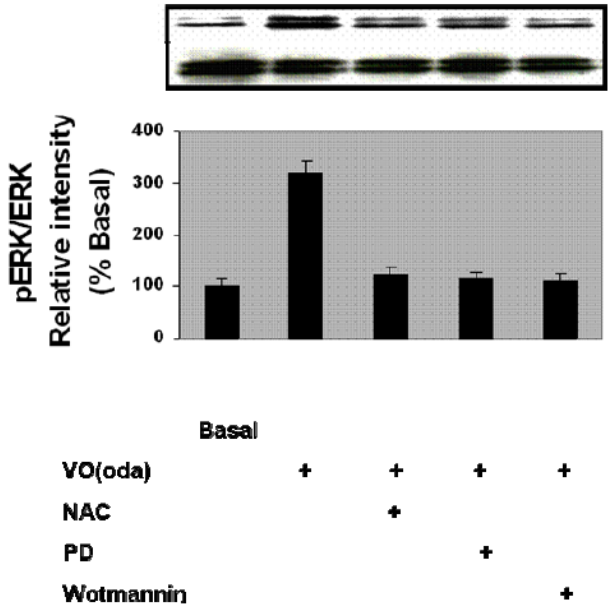

Fig. (16). Effect of inhibitors on VO(oda)-induced ERK-1/2 activation. UMR106 cells were pre incubated with 1 mM NAC during 1 h, 50 μM PD98059 or 10 μM wortmanin for 30 min. Then, the cells were incubated with 1mM VO(oda) during an additional hour. Relative intensity for ERK-1/2 stimulation was determined by densitometry. Results are expressed as % basal and are representative of three independent experiments, *significant difference vs. basal, $p<0.001$.

3. DISCUSSION AND CONCLUSIONS

Recent data suggest that under certain conditions, various metal cations may produce adverse effects in different cell types *in vivo* [47].

Strong chelating ligands are very important in aqueous systems since they are models for the trapping, transport and storage of different metallic species in living organisms [48]. Multidentate compounds of low molecular weight are of great interest for these processes since they bare functional groups with oxygen donor atoms such as carboxylates, hydroxamates and cathecolates [2, 3]. Oxodiacetate is a good model for the interactions of metals in living systems.

In the present study we investigated the effect of an organic derivative of vanadyl(IV) cation with oxodiacetate which is a model compound for the interaction of vanadium(IV) with biological ligands inside the cells. In a model of osteosarcoma and normal osteoblasts in culture, we found that the complex VO(oda) induced inhibition of cell proliferation. MC3T3-E1 cells showed more sensitivity to the vanadium complex than the tumoral osteoblasts [40]. Similar effects were previously reported by our group for other vanadium compounds [45, 49, 50]. Several mechanisms have been proposed to explain the cytotoxicity action of vanadium derivatives. We report herein the effects of VO(oda) on cell viability by NR assay, cell morphology, cytoskeleton architecture and putative mechanisms of cell death.

The NR technique is used to measure the growth of a population of cultured cells: viable cells take up the NR dye and transport it to a specific cellular compartment, the lysosomes. The uptake, transport, and storage of the NR dye require energy, as well as intact cellular and lysosomal structures [51]. Data presented herein show a cytotoxic effect of VO(oda) in a concentration-dependent manner in both cell lines. These results are in agreement with our previous report [40]. Moreover, decreased cell viability induced by vanadyl sulphate in tumorogenic and non-carcinogenic cells, [52] as well as the toxicity of vanadate solutions in cardiomyocytes [53] has been previously reported. Nevertheless, it could be observed that at low VO(oda) concentrations (5 and 10 μM), the NR assay showed an increase in the lysosomal activity in the normal osteoblasts. This behavior may be attributed to technical artifacts caused by vacuolization of the cytoplasm of cells such as it was reported in a model of RTgill-W1 cells [54] or to lysosomal swelling produced by weakly basic substances [55] or active osmotic agents [56]. On the other hand, the increment observed in the NR uptake at low doses may be also due to hormesis. This phenomenon consists in the stimulatory effect associated with low doses of a potentially toxic substance or stress [57]. A similar effect has been previously reported for different metal compounds [58-60].

Morphological alterations are good markers to infer the type of cell death (apoptosis or necrosis) induced by different chemical or physical agents. These changes vary among the different cell types due to their morphological, biochemical, and functional features. VO(oda) caused morphological alterations typical of apoptosis in both cell lines. They included cytoplasm and chromatin condensation, loss of cell connections and apoptotic bodies. The morphological changes in the cells intensified in a dose response manner

with great loss of cells and cellular structure at 100 μM of VO(oda). At this concentration we also found numerous dead cells detached from the extra cellular matrix (ECM), which correlated with the decrease in cell survival. Similar results have been previously reported for other vanadium compounds [17, 19, 51, 61] as well as for copper compounds [62]. Moreover, it has been shown that vanadium compounds may be responsible for the destruction of actin fibers [63, 64]. The organization of the cytoskeleton is essential for many cellular functions. One of the main components of the cytoskeleton ubiquitously distributed in the cells, are the actin filaments which are very sensitive to the action of different xenobiotics. These fibers determine the cellular shape and are involved in many cellular processes including signal transduction [65]. For this reason, changes in the cytoskeleton organization correlate with important consequences for cell survival [66] In the presence of VO(oda) it could be observed a significant reduction of actin fibers after 24 h of incubation. In addition at 100 μM of the complex, a complete cell decomposition manifested as scattered granular green color probably reflects actin cytoskeleton collapsing which is characteristic of apoptosis and is frequently observed at end-stage of this process [67, 68]. Besides, the disruption of actin network could cause damages to mitochondria membrane which consequently induce the activation of caspases and the down stream cleavage of proteins including actin [69]. Similar findings have been recently report for a vanadium(V) derivative [20].

It is well known that vanadium compounds exert their toxic effects through the generation of oxidative stress [12, 70 71].

In an attempt to better understand the possible mechanism involved in the cytotoxicity of VO(oda) in osteoblast-like cells, we evaluated the acute effect of this complex on the oxidative stress assessed by the oxidation of the probe DHR-123 and the ratio GSH/GSSG.

DHR-123 is a mitochondria-associated probe that selectively reacts with hydrogen peroxide [43, 44]. The complex VO(oda) increased ROS production in osteoblasts with a greater effect in the non transformed cell line (MC3T3-E1).

ROS formation enhanced by VO(oda) suggests that this effect was dependent on the cellular cell type. It was associated with cell death or membrane injury. The use of NAC diminished the level of ROS induced by the complex and allowed a better survival for the cells. This observation was in agreement with previous results from our laboratory on the action of vanadate and vanadyl(IV) cation in the model of osteoblasts in culture [45] as well as in a model of macrophage cells in culture [72].

GSH is one of the mayor reducing agents in mammalian cells. This thiol acts by sequestering free radicals and also maintains the cellular redox status through the balance of the couple GSH/GSSG [28, 73]. Exposure to ROS, can increase the content of GSH by increasing the rate of GSH synthesis as it was reported for some systems. [28] Nevertheless, a sustained ROS accumulation may cause an accumulation of GSSG inside the cells. Because of this, the GSH/GSSG ratio is a good marker of the oxidative stress [74, 75].

In osteoblast-like cells, VO(oda) induced a decrease in the GSH/GSSG ratio at 50 and 100 μM. This decrease was due to the accumulation of GSSG and the lowering of GSH levels. However, the total glutathione pool (reduced plus oxidized forms) was not affected, as it was previously reported for vanadium metavanadate in peritoneal macrophages of mice [76] These results denoted that the depletion of GSH concentration would mediate the cytotoxic action of VO(oda). On the other hand, the fact that UMR106 osteosarcoma cells have approximately twice the GSH concentration than MC3T3-E1 cells, may reflect a better adaptation of the tumoral cells to oxidative stress and explain the reason of the less sensitivity of these cells towards the deleterious effects of VO(oda). Besides, when the osteoblasts were subjected to a strong oxidative pressure (200 μM VO(oda)), the results of time course experiments revealed that the tumoral osteoblasts were able to increase GSH/GSSG ratio after 4 h while this effect could not be observed in the normal osteoblasts. We confirm that the depletion of GSH played a crucial role in the cytotoxic effect of the complex since the use of BSO reinforced the deleterious action of VO(oda). Besides, when a proliferation experiment was carried out in the presence of the complex plus GSH, a complete inhibition of the antiproliferative effect could be observed in both cell lines.

Mitochondrias are one of the more important organelles that can regulate cellular apoptosis [77, 78]. The mitochondria transmembrane potencial maintains the integrity and functions of the mitochondrias. Dissipation of the MMP can lead the cells into apoptosis or necrosis [79]. The disruption of MMP alters the permeability of mitochondria membrane promoting the release of apoptogenic factors such as the cytochrome c and subsequent activation of caspases [80].

One of the most used probes for the determination of MMP is Rhodamine 123. It is a lipofilic and low toxicity compound with high affinity for mitochondria [81, 82]. Vanadate induced the loss of MMP through the generation of H_2O_2 in mouse epidermal cells, promoting the death by apoptosis [83]. Similar results were reported by D´Cruz *et al*. for vanadocenes in germinal cells [84, 85].

In our model system, VO(oda) also caused a dissipation of MMP in both cell lines in a dose dependent trend. This effect was prevented by GSH addition confirming that the MMP alteration was produced by oxidative stress.

ERK pathway is classically recognized as a key transducer in the signal cascade mediating cell proliferation and differentiation [86]. Nevertheless, recent investigations have shown that the ERK pathway also mediates cell cycle arrest, antiproliferation and apoptotic and non-apoptotic death [87]. It has been previously reported that vanadium compounds are able to activate this pathway [22, 86, 88].

To get a deeper insight in the mechanisms involved in the action of VO(oda), we studied the relationship between ERK pathway activation induced by the complex. As ERK activation is a fast and transient process, we assessed the effects of vanadium in the range of 100-1000 μM during 1 h incubation, as it has been previously reported [89]. A dose-dependent increase in ERK phosphorylation was observed in osteoblast-cell lines. According with our results VO(oda)

activated this pathway through two mechanisms. One of them was dependent on oxidative stress as it was proven by the effect of NAC which inhibited the activation caused by the complex. The second mechanism involved in the activation of ERKs was mediated by the MEK and PI3-K cascades as it was demonstrated by the inhibitory effects of wortmanin and PD98059. To test if these two mechanisms of ERK activation played a role in VO(oda) cytotoxicity, proliferative assays were performed pre-incubating the cells with the inhibitors *prior* the addition of the complex. Wortmanin and PD98059 could not prevent the deleterious action of VO(oda). On the contrary, NAC caused a partial protection in the osteoblasts, suggesting that ERK activation by oxidative stress may be responsible, at least partially, for VO(oda) cytotoxicity in osteoblast-like cells.

To conclude, we propose the following model on the putative mechanisms of VO(oda) cytotoxicity in osteoblast-like cells (Fig. **17**). According to this model, once the complex enters the cells it promotes the generation of ROS mainly in the mitochondrias. The increment in ROS levels would be the cause of a decrease of GSH concentration, alteration of the intracellular redox balance (GSH/GSSG) and the disassembling of actin filaments. Besides, the oxidative stress causes a dissipation of MMP which would be a "point of not return" that leads the cells to apoptosis. On the other hand, VO(oda) promotes an oxidative phosphorylation of ERK pathway which seems to be also partially involved in apoptotic events.

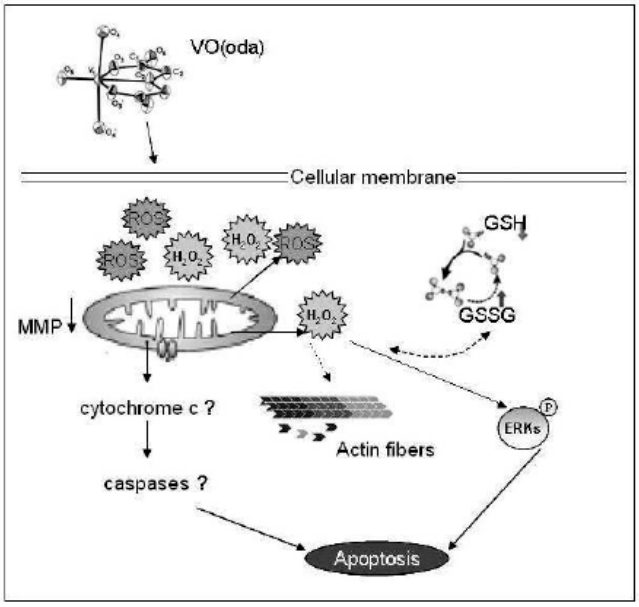

Fig. (17). Schematic putative mechanisms of cytotoxicity induced by VO(oda) in osteoblasts in culture.

4. EXPERIMENTAL SECTION

4.1. Materials

VO(oda) (97% purity determined by thermal analysis) was kindly provided by Prof. Dr Baran (UNLP, La Plata, Argentina), and it was synthesized and characterized according to literature [39] Tissue culture materials were purchased from Trading New Technologies (Buenos Aires, Argentina). Dulbecco´s Modified Eagles Medium (DMEM), fetal bovine serum (FBS) from GBO Argentina S.A (Buenos Aires, Argentina); trypsin-EDTA was provided by Gibco (Gaithersburg, Md, USA); Rhodamine 123, GSH, GSSG, neutral red, wortmannin, BSO and NAC were purchased from Sigma Chemical Co. (St. Louis, MO, USA). PD98059 was from Calbiochem (USA and Canada). An ECL kit was provided by Amersham Life Sciences (USA). Dihydrorhodamine 123 (DHR) was from Molecular Probes (Eugene, OR, USA). The specific rabbit polyclonal antibody IgG anti-ERK (K-23), mouse monoclonal anti-PERK (E-4), anti rabbit IgG-HRP and antimouse IgG-HRP were purchased from Santa Cruz Biotechnology (Santa Cruz, CA, USA). Phalloidin was from Invitrogen Corporation (Buenos Aires, Argentina).

4.2. Methods

4.2.1. Preparation of VO(oda) Solutions

Fresh stock solutions of the complex and the free ligand were prepared in distilled water at 100 mM and diluted according to the concentrations indicated in the legends of the figures.

4.2.2. Cell Culture and Incubations

MC3T3-E1 mouse calvaria-derived osteoblasts and UMR106 rat osteosarcoma cells were grown in DMEM containing 10 % FBS, 100 U/ml penicillin and 100 µg/ml streptomycin at 37º C in 5% CO_2 atmosphere.

Cells were seeded in a 75 cm^2 flask and when 70-80 % of confluence was reached, cells were subcultured using 0.1% trypsin- 1 mM EDTA in a Ca^{2+} -Mg $^{2+}$ free phosphate buffered saline (PBS). For experiments, cells were grown in multi-well plates. When cells reached the desired confluence, the monolayers were washed with DMEM and were incubated under different conditions according to the experiments.

4.2.3. Cell Proliferation: Crystal Violet Assay

A mitogenic bioassay was carried out as described by Okajima *et al.* [90] with some modifications. Briefly, cells were grown in 48 well plates. When cells reached 70% confluence, the monolayers were washed twice with serum-free DMEM and incubated with medium alone (basal) and different concentrations (10-100µM) of the complex or the free ligand. Besides, incubations were also carried out with the complex plus NAC, BSO, GSH, PD98059 and wortmannin. Cells were pre-incubated with the following doses of the mentioned inhibitors for different periods previous to the addition of different concentrations of the complex: NAC (100 µM for MC3T3-E1 osteoblasts and 200 µM for UMR106 cells) during 2 h. To select the optimal NAC concentration for each cell line, osteoblasts were incubated with different concentrations of NAC in presence of 50 µM de VO(oda) for 24h. At the end, proliferative assays were carried out. NAC concentrations which produced maximal inhibition of the antiproliferative action of the complex were chosen for the experiments. Besides, the following inhibitors were used for both cell lines: BSO (10 µM for MC3T3-E1 osteoblasts and 40 µM for UMR106 cells, overnight), GSH

(3 mM for MC3T3-E1 cells and 1 mM for the tumoral UMR106 osteoblasts, for 2 h in both cell lines), PD98059 (1-20 μM) and wortmannin (0.25-10 μM) for 30 min in both cell lines. Following these pre-incubations, different concentrations of VO(oda) were added for 24 h at 37º C. After this treatment, the monolayers were washed with PBS and fixed with 5% glutaraldehyde/PBS at room temperature for 10 min. After that, they were stained with 0.5% crystal violet / 25% methanol for 10 min. Then, the dye solution was discarded and the plate was washed with water and dried. The dye taken up by the cells was extracted using 0.5 ml/well 0.1 M glycine/HCl buffer, pH 3.0 / 30% methanol and transferred to test tubes. Absorbance was read at 540 nm after a convenient sample dilution. It was previously shown that under these conditions, the colorimetric bioassay strongly correlated with cell proliferation measured by cell counting in Neubauer chamber [49, 61].

4.2.4. Neutral Red Assay

The neutral red accumulation assay was performed according to Borenfreund and co-workers [51] Cells were plated in 96 well culture plates (2.5×10^4 UMR106cells/well or 1.8×10^4 MC3T3-E1 cells/well). Cells were treated with different VO(oda) concentrations for 24 h at 37°C in 5% CO_2 in air. After treatment, the medium was replaced by one containing 100 μg/ml Neutral Red (NR) dye and cells were incubated for other 3 h. Then, neutral red medium was discarded, the cells were rinsed twice with warm (37°C) PBS (pH 7.4) to remove the non-incorporated dye, and 100 μl of 50% ethanol, 1% acetic acid solution was added to each well to fix the cells releasing the neutral red into solution. The plates were shaken for 10 min, and the absorbance of the solution in each well was measured in a Microplate Reader (7530, Cambridge technology, Inc, USA) at 540 nm, and compared with wells with untreated cells. Optical density was plotted as percent of control.

4.2.5. Cell Morphology

Cells were grown on glass coverslips and incubated under control conditions (without complex addition) or with different concentrations of VO(oda) in serum-free DMEM for 24 h. Then, the cells were fixed and stained with Giemsa [45, 62]. Samples were observed under light microscopy.

4.2.6. Cytoskeleton Actin Determination

A fluorescence technique was used to visualize actin cytoskeleton filaments. Cells were grown on glass coverslips until a 70 % of confluence; after that the cells were incubated for 24 h at 37 °C with different concentrations of VO(oda). Then, the cells were fixed, permeabilized during 4 min at room temperature using absolute ethanol (cold at – 20 ºC), washed with PBS and blocked with non-fat milk for 2 h. After washing, the cells were incubated with FITC-phalloidin for 2 h. The samples were washed twice and mounted in slides. Labeled cells with green fluorescence were observed using a fluorescence microscope.

4.2.7. Reversibility Assay

This assay determines the toxicity of an exogenous agent measured through the viability of the cells after stress incubation. Cells were cultured in 48 well dishes to 70% confluence. Then, they were incubated with different concentrations of VO(oda) at 37°C for 24 h. After that, 24 wells were used to evaluate cell proliferation by the crystal violet assay. The other 24 wells were washed to eliminate the conditioned medium with the complex and then were incubated with DMEM supplemented with FBS. After that, these cells were incubated for another 24 h at 37°C. Finally, cell proliferation was determined by the crystal violet assay.

4.2.8. Determination of Reactive Oxygen Species (ROS) Production

The possible VO(oda) –induced oxidative stress in the osteoblasts was evaluated by measurement of intracellular production of reactive oxygen species (ROS) after incubation of the cell monolayers with different concentrations of the complex during 4 hours at 37 ºC. ROS generation was determined by oxidation of DHR-123 to rhodamine by spectrofluorescence as we have previously described [45]. NAC was used to evaluate the role of the oxidative stress in the complex cytotoxicity under similar concentrations and incubation time to those employed in the crystal violet assay.

4.2.9. Fluorometric determinAtion of Cell GSH and GSSG Levels

GSH and GSSG levels were determined in osteoblasts in culture as follows. Confluent osteoblast monolayers from 24 well dishes were incubated with different doses of VO(oda) for 24 h at 37ºC. Then, the monolayers were washed with PBS and harvested by incubating with 250 μL Triton 0.1% for 30 min. For GSH determination, 100 μL aliquots were mixed with 1.8 mL of ice cold phosphate buffer (Na_2HPO_4 0.1 M-EDTA 0.005 M pH 8) and 100 μL o-phthaldialdehyde (0.1 % in methanol) as it was described by Hissin and Hilf [91]. For the determination of GSSG, 100 μL aliquots were mixed with 1.8 mL NaOH 0.1 M and o-phthaldialdehyde as before. Previously, to avoid GSH oxidation the cellular extracts for GSSG determination were incubated with 0.04 M of N-ethylmaleimide (NEM). Fluorescence at an emission wavelength of 420 nm was determined after excitation at 350 nm. Standard curves with different concentrations of GSH or GSSG were processed in parallel. Protein content in each cellular extract was quantified using Bradford assay [92]. The ratio GSH/GSSG was calculated as % basal for all the experimental conditions. For time course experiments, the osteoblasts were incubated with 200 μM VO(oda) during different periods (0-240 min) and then we proceeded as described above.

4.2.10. Activation of Erk Pathway: Western Blot Analysis

The activation status of the ERK-1/2 transduction pathway induced by VO(oda) was evaluated by Western blot [46]. In these experiments, osteoblastic cells growing in serum free medium with the addition of different concentrations of VO(oda) alone or VO(oda) plus PD98059, wortmannin and NAC for different periods according to the figure legends. The cells were washed twice with cold PBS and lysated in Laemmli's buffer [93]. These lysates were heated at 100 º C for 3 min and aliquots were subjected to 12 % SDS-PAGE. The separated proteins were then electrotransferred to nitrocellulose membranes. After washing and

blocking, the membranes were incubated with a monoclonal anti pERK antibody, or a polyclonal antibody that recognizes both phosphorylated and non- phosphorylated ERK-1/2. Blots were developed using chemioluminiscence reagents. The intensity of the specific bands was quantified by densitometry after scanning of the photographic films. Images were analyzed using the Scion-beta 2 program.

4.2.11. Mitochondrial Membrana Potencial (MMP) Measurement

Rhodamine 123, a fluorescent probe, was used to detect alterations in MMP. Cells were cultured in 6 well dishes at 37 °C. When the monolayer reached 70% confluence, the medium was replaced by DMEM without BFS and with addition of different doses of VO(oda) or 100 µM VO(oda) plus 3 mM GSH for MC3T3-E1 cells and 1 mM GSH for UMR106 cells. After this treatments, the cells were incubated with Rh123 (5 µg/mL final concentration) at 37 °C for 30 min. Adherent cells were washed twice with PBS and harvested by a brief trypsinization followed by another wash with PBS. The changes in MMP were analyzed by flow cytometry with the single beam at 488 nm excitation wave length and 530 nm emission wave lengths [94]. The results were analyzed by FCS Express software.

4.2.12. Statistical Analysis

For statiscal analysis the following methods were used: One-way ANOVA followed by Newman-Keuls test for comparison of the differences and the Student *t* test for the comparison of two means Results represent the mean ± SEM. All the results with $p<0.05$ were considered statistically significant.

ACKNOWLEDGEMENTS

This work was supported by UNLP and CONICET (PIP 6366). DAB, CIM and SBE are members of the Carrera del Investigador, CONICET, Argentina. ALDV is a postdoctoral fellowship from CONICET, Argentina. JR is a doctoral fellowship from CONICET, Argentina.

REFERENCES

[1] Harding, M.M.; Mokdsi, G. Antitumor metallocenes: structure-activity studies and interactions with biomolecules. *Curr. Med. Chem.* **2000**,**7**, 1289–1303.

[2] Lippard, S.J. and Berg, J. M. (1994) Principles of Bioinorganic Chemistry. University Science Books, Mill Valley, CA.

[3] Costas, M.; Mehn, M.P.; Jensen, M.P.; Que L. Jr. Dioxygen activation at mononuclear nonheme iron active sites: enzymes, models, and intermediates. *Chem Rev*. **2004,** 104, 939-86.

[4] Baggio, R.; Garland, M. T.; Perec, M. Acta Crystallographica Section C.Crystal Structure Communications Volume 59, Part 1 (January 2003).

[5] Chao, J.; Xiang, Z.; Zhao-Peng, Y.; Zhi-Yong, W. Molecular chains: two new isomorphous coordination polymers of oxydiacetate. *Inorg. Chem. Comm.* **2003**, 6, 706–709.

[6] Nielsen, F.H. Vanadium in mammalian physiology and nutrition. *In* Sigel H, Sigel A, Biological systems, New eds. Metal Ions in Biological Systems. New York, Marcel Dekker, **1995**, 31, 543–574.

[7] Baran, E. Some contributions to the bioinorganic chemistry of vanadium. *Anal Acad Nac Cs Fis Nat. Buenos Aires* 1996, 46, 35-43

[8] Upreti, R.K. Membrane–vanadium interaction: a toxicokinetic evaluation. *Mol Cell Biochem* **1995**, 153, 167–171.

[9] Morinville, A.; Maysinger, D.; Shaver, A. From Vanadis to Atropos: vanadium compounds as pharmacological tools in cell death signalling. *Trends Pharmacol. Sci.* **1998**, 19, 452–460.

[10] Thompson, K.H.; McNeill, J.H.; Orvig, C. Vanadium Compounds as Insulin Mimics. ***Chem. Rev.*** 1999, **99** (9), 2561–2572.

[11] Djordjevic, C. Antitumor activity of vanadium compounds. *Met Ions Biol Syst*. **1995**, 31, 595–616.

[12] Evangelou, A.M. Vanadium in cancer treatment. *Crit Rev Oncol Hematol* 2002, 42, 249–265.

[13] Hasenknopf, B. Polyoxometalates: introduction to a class of inorganic compounds and their biomedical applications. *Front Biosci*. **2005**, 10, 275-87.

[14] Cortizo, A.M.; Molinuevo, M.S.; Barrio, D.A.; Bruzzone, L. Osteogenic activity of vanadyl(IV)-ascorbate complex: evaluation of its mechanism of action. *Int J Biochem Cell Biol*. **2006**, 38, 1171–1180.

[15] Barrio, D.A.; Cattáneo, E.R.; Apezteguía, M.C.; Etcheverry, S.B. Vanadyl(IV) complexes with saccharides. Bioactivity in osteoblast-like cells in culture. *Can J Physiol Pharmacol* **2006**, 84, 765–775.

[16] Etcheverry, S.B.; Barrio, D.A. In: *Vanadium: the Versatile Metal* Chapter 15, K. Kustin, J. Pessoa and D.C. Crans, Editors, American Chemical Society, Washington DC (2007), pp. 204–216.

[17] Molinuevo, M.S.; Barrio, D.A.; Cortizo, A.M.; Etcheverry, S.B. Antitumoral properties of two new vanadyl(IV) complexes in osteoblasts in culture: role of apoptosis and oxidative stress. *Can. Chem.Pharmacol*. **2004**, 53,163–172.

[18] Molinuevo, M.S.; Cortizo, A.M.; Etcheverry, S.B. Vanadium(IV) complexes inhibit adhesion, migration and colony formation of UMR106 osteosarcoma cells. *Can. Chem. Pharmacol.* 2008, 61, 767-73.

[19] Etcheverry, S.B.; Ferrer, E.G.; Naso, L.; Rivadeneira, J.; Salinas, V.; Williams, P.A.M. Antioxidant effects of the VO(IV) hesperidin complex and its role in cancer chemoprevention. *J Biol Inorg Chem*. **2008,** 13, 435-447.

[20] Rivadeneira, J.; Barrio, D.A.; Arrambide, G.; Gambino, D.; Bruzzone, L.; Etcheverry, S.B. Biological effects of a complex of vanadium(V) with salicylaldehyde semicarbazone in osteoblasts in culture: mechanism of action. *J Inorg Biochem*. **2009,** 103, 633-642.

[21] Gresser, M.; Tracey, A.S. In: N.D. Chasteen, Editor, *Vanadium in Biological Systems*, Kluwer Academic Press, Dordrecht 1990, pp. 63–79.

[22] Pandey, S..K.; Theberge, J.F.; Bernier, M.; Srivastava, A.K. Phosphatidylinositol 3-kinase requirement in activation of the ras/c-raf-l/MEK/ERK and p70 (s6k) signaling cascade by the insulinomimetic agent vanadyl sulfate. *Biochemistry* **1999**, 38, 14667–14675.

[23] Rumora, L.; Hadzija, M.; Maysinger, D.; Zanić-Grubisić, T. Positive regulation of ERK activation and MKP-1 expression by peroxovanadium complex bpV (phen). *Cell Biol. Toxicol.* **2004** 20(5), 293-301.

[24] Théberge, J.F.; Mehdi, M.Z.; Pandey, S.K.; Srivastava, A.K. Prolongation of insulin-induced activation of mitogen-activated protein kinases ERK 1/2 and phosphatidylinositol 3-kinase by vanadyl sulfate, a protein tyrosine phosphatase inhibitor. *Arch. Biochem. Biophys.* **2003,** 420(1), 9-17.

[25] Cortizo, A.M.; Kreda, S.M. In: J.A. Centeno, P.H. Collery, G. Vernet, R.B. Finkelman, H. Gibb and J.C. Etienne, Editors, *Metal Ions in Biology and Medicine* vol. 6, Jhon Libbey, Eurotext, Paris 2000, pp. 714–716.

[26] Ye, J.; Ding, M.; Zhang, X.; Rojanasakul, Y.; Nedospasov, S.; Vallyathan, V.; Castranova, V.; Shi, X. Induction of TNF alpha in macrophages by vanadate is dependent on activation of transcription factor N-F-kappa B and free radical reactions. *Mol. Cell. Biochem.* **1999**, 198, 193–200.

[27] Narla, R.K.; Dong, Y.; Klis, D.; Uckun, F.M. *In vivo* antitumor activity of bis(4,7-dimethyl-1,10-phenanthroline) sulfatooxovanadium(IV) (METVAN [VO(SO4)(Me2-Phen)2]). *Clin. Cancer Res.* 2001, 7, 1094–1110.

[28] Valko, M.; Rhodes, C.J.; Moncol, J.; Izakovic, M.; Mazur M. Free radicals, metals and antioxidants in oxidative stress-induced cancer. *Chem. Biol.Interact.* **2006**, 160, 1-40.

[29] Reed, D. J.; Fariss, M. W. Glutathione depletion and susceptibility. *Pharmacol. Rev*. **1984**, 36, 25- 33.

[30] Mohamadin, A.M.; Hammad, L.A.; El-Bab, M.; Abdel Gawad, H.S. Attenuation of oxidative stress in plasma and tissues of rats with experimentally induced hyperthyroidism by caffeic Acid

phenylethyl ester. *Basic Clin. Pharmaco. Toxico*. **1996**, 100, 84–90.

[31] Chen, F.; Vallyathan, V.; Castranova, V.; Shi, X. Cell apoptosis induced by carcinogenic metals. *Mol. Cell. Biochem*. **2001**, 222(1-2).183-8.

[32] Sakurai, H. Vanadium distribution in rats and DNA cleavage by vanadyl complex: Implication for vanadium toxicity and biological effects *Environ. Health Perspect.* **1994**, 3, 35–36.

[33] Ivancsits, S.; Pilger, A.; Diem, E.; Schaffer, A.; Rüdiger, H. Vanadate induces DNA strand breaks in cultured human fibroblasts at doses relevant to occupational exposure. *Mutat. Res.* **2002**, 519, 25–35.

[34] Jelikić-Stankov, M.; Uskoković-Marković, S.; Holclajtner-Antunović, I.; Todorović, M.; Djurdjević, P. Compounds of Mo, V and W in biochemistry and their biomedical activity. *J. Trace Elem. Med. Biol*. **2007**; 21(1), 8-16.

[35] Domingo, J.L. Vanadium: A review of the reproductive and developmental toxicity. *Reprod. Toxicol.* **1996**, 10 175–182.

[36] Sabbioni, E.; Pozzi, G.; Devos, S.; Pintar, A.; Casella, L.; Fischbach, M. The intensity of vanadium(V)-induced cytotoxicity and morphological transformation in BALB/3T3 cells is dependent on glutathione-mediated bioreduction to vanadium(IV)). *Carcinogenesis* **1993**, 14, 2565–2568.

[37] Kordowiak, A.M.; Klein, A.; Goc, A.; Dabroś, W. Comparison of the effect of VOSO4, Na3VO4 and NaVO3 on proliferation, viability and morphology of H35-19 rat hepatoma cell line. *Pol. J. Pathol.* **2007**; 58(1), 51-57.

[38] Altamirano-Lozano, M. Genotoxic effects of vanadium compounds. *Invest.* Clin. **1998**, 39, 39-47.

[39] Del Río, D.; Galindo, A.; Vicente, R.; Mealli, C.; Ienco, A.; Masi, D. Synthesis, molecular structure and properties of oxo vanadium(IV) complexes containing the oxydiacetate ligand**.** *Dalton Trans*. **2003**, 1813 – 1820.

[40] Rivadeneira, J.; Barrio, D.A.; Etcheverry, S.B.; Baran, E.J. Spectroscopic characterization of a VO2+ complex of oxodiacetic acid and its bioactivity on osteoblast-like cells in culture**.** *Biol. Trace Elem. Res.* **2007,** 118, 159–166.

[41] Del Río, D.; Galindo, A.; Tejedo, J.; Bedoya, F.J.; Ienco, A.; Mealli, C**.** Synthesis, antiapoptotic biological activity and structure of an oxo–vanadium(IV) complex with an OOO ligand donor set. *Inorg. Chem. Comms.* **2000**, 3(1), 32-34.

[42] Royall, J.A.; Ischiropoulos, H. Evaluation of 2′,7′-dichlorofluorescin and dihydrorhodamine 123 as fluorescent probes for intracellular H_2O_2 in cultured endothelial cells. *Arch. Biochem. Biophys.* **1993**, 302, 348–355.

[43] Capella. M.A.M.; Capella, L.S.; Valente, R.C.; Gefé, M.; Lopes, A.G. Vanadate-induced cell death is dissociated from H_2O_2 generation. *Cell Biol. Toxicol.* **2007**, 23, 413–420.

[44] Qin, Y.; Lu, M.; Gong, X. Dihydrorhodamine 123 is superior to 2,7-dichlorodihydrofluorescein diacetate and dihydrorhodamine 6G in detecting intracellular hydrogen peroxide in tumor cells. *Cell Biol. International* **2008**, 32, 224-228.

[45] Cortizo, A.M.; Bruzzone, L.; Molinuevo, M.S.; Etcheverry, S.B. A possible role of oxidative stress in the vanadium-induced cytotoxicity in the MC3T3E1 osteoblast and UMR106 osteosarcoma cell lines. *Toxicology.* **2000**, 147, 89–99.

[46] Barrio, D.A.; Williams, P.A.M.; Cortizo, A.M.; Etcheverry, S.B. Synthesis of a new vanadyl(IV) complex with trehalose (TreVO): insulin-mimetic activities in osteoblast-like cells in culture. *J Biol. Inorg. Chem*. **2003**, 8, 459–468.

[47] Schedle, A.; Samorapoompichit, P.; Rausch-Fan, X.H.; Franz, A.; Füreder, W.; Sperr, W.R.; Sperr, W.; Ellinger, A.; Slavicek, R.; Boltz-Nitulescu, G.; Valent. Response of L-929 fibroblasts, human gingival fibroblasts, and human tissue mast cells to various metal cations. *J. Dent. Res*. **1995**, 74(8), 1513-20.

[48] Harding, C.J.; Henderson, R.K.; Powell, A.K. A new type of hexanuclear iron(III) hydroxo(oxo) cluster. Angewandte Chemie. International edition in English. *Angew. Chem., Int. Ed. Engl*. **1993**, 32, 570-572.

[49] Cortizo, A.M.; Etcheverry, S.B. Vanadium derivatives act as growth factor—mimetic compounds upon differentiation and proliferation of osteoblast-like UMR106 cells. *Mol. Cell Biochem*. **1995**, 145, 97–102

[50] Sálice, V.C.; Cortizo, A.M.; Gomez Dumm, C.L.; Etcheverry, S.B. Tyrosine phosphorylation and morphological transformation induced by four vanadium compounds on MC3T3E1 cells. *Mol. Cell. Biochem.* **1999**, 198, 119–128.

[51] Borenfreund, E.; Puerner, J.A. A simple quantitative procedure using monolayer culture for toxicity assays. *J. Tissue Cult. Methods*. **1984**, 9, 7-9.

[52] Holko, P.; Ligeza, J.; Kisielewska, J.; Kordowiak, A.M.; Klein A. The effect of vanadyl sulphate (VOSO4) on autocrine growth of human epithelial cancer cell lines. *Pol. J. Pathol.* **2008,** 59(1), 3-8.

[53] Soares, S.S.; Henao, F.; Aureliano, M.; Gutiérrez-Merino, C. Vanadate induces necrotic death in neonatal rat cardiomyocytes through mitochondrial membrane depolarization. *Chem. Res. Toxicol*. **2008**, 21(3), 607-18.

[54] Dayeh, V.R.; Schirmer, K.; Bols, N.C. Ammonia-containing industrial effluents, lethal to rainbow trout, induce vacuolisation and Neutral Red uptake in the rainbow trout gill cell line, RTgill-W1. *Altern. Lab. Anim*. **2009**, 37(1), 77-87.

[55] Ohkuma, S.; Poole, B. Cytoplasmic vacuolation of mouse peritoneal macrophages and the uptake into lysosomes of weakly basic substances. *J.Cell Biol*. **1981**, 90, 656-664.

[56] Olivier, P.; Testard, P.; Marzin, D.; Abbott, D. Effect of high polyol concentrations on the neutral red absorption assay and tetrazolium-MTT test of rat hepatocytes in primary culture. *Toxicol. in Vitro.* **1995**, 9, 133-138.

[57] Lefcort, H.; Freedman, Z.; House, S.; Pendleton, M. Hormetic effects of heavy metals in aquatic snails: is a little bit of pollution good? *Ecohealth.* **2008**, 5(1), 10-7.

[58] Schmidt, C.M.; Cheng, C.N.; Marino, A.; Konsoula, R.; Barile F.A. Hormesis effect of trace metals on cultured normal and immortal human mammary cells*. Toxicol. Ind. Health.* **2004**, 20(1-5), 57-68.

[59] Perez-Benito, J.F. Effects of chromium(VI) and vanadium(V) on the lifespan of fish.. *J.Trace Elem. Med. Biol.* **2006**, 20(3), 161-70.

[60] Stebbing, A.R. Tolerance and hormesis--increased resistance to copper in hydroids linked to hormesis. *Mar. Environ. Res.* **2002**, 54(3-5), 805-809.

[61] Etcheverry, S.B.; Crans, D.C.; Keramidas, A.D.; Cortizo, A.M. Insulin-mimetic action of vanadium compounds on osteoblast-like cells in culture. *Arch Biochem. Biophys.* **1997**, 338, 7-14.

[62] Etcheverry, S.B.; Ferrer, E.G.; Naso, L.; Barrio, D.A.; Lezama, L.; Rojo, T.; Williams, P.A.M. Losartan and its interaction with copper(II): Biological effects. *Bioorg. Med. Chem.* **2007**, 15, 6418–6424.

[63] Luber, B.; Candidus, S.; Handschuh, G.; Mentele, E.; Hutzler, P.; Feller, S.; Voss, J.; Höfler, H.; Becker, K.F. Tumor-derived mutated E-cadherin influences beta-catenin localization and increases susceptibility to actin cytoskeletal changes induced by pervanadate. *Cell Adhes. Commun*. **2000**, 7(5), 391-408.

[64] Yang, X.G.; Yang, X.D.; Yuan, L.; Wang, K.; Crans, D.C. The permeability and cytotoxicity of insulin-mimetic vanadium compounds. *Pharm. Res.* **2004,** 21, 1026–1033.

[65] Stossel, T.P. From signal to pseudopod. How Cells control cytoplasmic actin assembly**.** *J. Biol. Chem.* **1989**, 5 18261–18264.

[66] Osin´ska-Kro´licka; Podsiadly, H.; Bukietyn´nska, K.; Zemanek-Zboch, M.; Nowak D.; Suchoszek-Lukaniuk, K.; Malicka-Blaszkiewicz, M. Vanadium(III) complexes with l-cysteine – stability, speciation and the effect on actin in hepatoma Morris 5123 cells. *J. Inorg. Biochem.* **2004**, 98, 2087–2098.

[67] Hacker, G. The morphology of apoptosis. *Cell Tissue Res*. **2000**, 301, 5–17.

[68] Yuana, B.; Jefferson, A.M.; Millecchia, L.; Popescu, N.C.; Reynolds, S.H. Morphological changes and nuclear translocation of DLC1 tumor suppressor protein precede apoptosis in human non-small cell lung carcinoma cells. *Exp. Cell Res*. **2007**, 313, 3868 – 3880.

[69] Yamazaki, Y.; Tsuruga, M.; Zhou, D.; Fujita, Y.; Shang, X.; Dang, Y.; Kawasaki, K.; Oka, S. Cytoskeletal disruption accelerates caspase-3 activation and alters the intracellular membrane reorganization in DNA damage-induced apoptosis. *Exp. Cell Res*. **2000**, 259, 64-78.

[70] Ye, J.; Ding, M.; Leonard, S.S.; Robinson, V.A.; Millecchia, L.; Zhang, X.; Castranova, V.; Vallyathan, V.; Shi, X. Vanadate induces apoptosis in epidermal JB6 P+ cells via hydrogen peroxide-mediated reactions. *Mol. Cell Biochem*. **1999**, 202, 9-17.

[71] Zhang, Z.; Huang, C.; Li, J.; Leonard, S.S.; Lanciotti, R.; Butterworth, L.; Shi, X. Vanadate-infuced cell growth regulation and the role of reactive oxygen species. *Arch. Biochem. Biophys*. **2001**, 392, 311-320.

[72] Molinuevo, M.S.; Etcheverry, S.B.; Cortizo, A.M. Macrophage activation by a vanadyl-aspirin complex is dependent on L-type calcium channel and the generation of nitric oxide. *Toxicology*, **2005**, 210, 205–212

[73] Jones, D.P., Carlson, J.L.; Mody, V.C.; Cai, J.Y.; Lynn, M.J.; Sternberg, P. Redox state of glutathione in human plasma. *Free Rad. Biol. Med.* **2000**, 28, 625-635.

[74] Hwang, C.; Sinskey, A.J.; Lodish, H.F. Oxidized redox state of glutathione in the endoplasmic-reticulum. *Science.* **1992**, 57, 1496–1502.

[75] Giovannini, C.; Scazzocchio, B.; Matarrese, P.; Varì, R.; D'Archivio, M.; Di Benedetto, R.; Casciani, S.; Dessì, M.R.; Straface, E.; Malorni, W.; Masella, R. Apoptosis induced by oxidized lipids is associated with up-regulation of p66Shc in intestinal Caco-2 cells: protective effects of phenolic compounds. *J Nutr. Biochem*. **2008**, 19,118-28.

[76] Cohen, M.D.; Wei, C.I. Effects of ammonium metavanadate treatment upon macrophage glutathione redox cycle activity, superoxide production, and intracellular glutathione status. *J Leukoc. Biol.* **1988**, 44,122-129.

[77] Herr, I.; Debatin, K.M. Cellular stress response and apoptosis in cancer therapy. *Blood*. **2001**, 98, 2603-2614.

[78] Grebenova, D.; Kuzelova, K.; Smetana, K.; Pluskalova, M.; Cajthamlova, H.; Marinov, I.; *et al.* Mitochondrial and endoplasmic reticulum stress-induced apoptotic pathways are activated by 5-aminolevulinic acid-based photodynamic therapy in HL60 leukemia cells. *J. Photochem. Photobiol. B*. **2003**, 69, 71-85.

[79] Mayer, B.; Oberbauer, R. Mitochondrial regulation of apoptosis. *News Physiol. Sci.* **2003**, 18, 89-94.

[80] Kim, R.; Tanabe, K.; Uchida, Y.; Emi, M.; Inoue, H.; Toge, T. Current status of the molecular mechanisms of anticancer drug-induced apoptosis. The contribution of molecular-level analysis to cancer chemotherapy. *Cancer Chemother Pharmacol.* **2002**, 50, 343-352.

[81] Darzynkiewicz, Z.; Traganos, F.; Staiano-Coico, L.; Kapuscinski, J.; Melamed, M.R.; Interaction of rhodamine 123 with living cells studied by flow cytometry. *Cancer Res* **1982**, 42, 799-806.

[82] Lopez-Mediavilla, C.; Orfao, A.; Garcia, M.V.; Medina, J.M.. Changes in adult rat liver mitochondrial populations at different energy states analyzed by flow cytometry. *Biochim. Biophys. Acta.* **1995**, 1232, 27-32.

[83] Huang, C.; Zhang, Z.; Ding, M.; Li, J.; Ye, J. *et al.* Vanadate induces p53 transactivation through hydrogen peroxide and causes apoptosis. *J. Biol. Chem*. **2000**, 275 32516–32522.

[84] D'Cruz, O.J.; Ghosh, P.; Uckun, F.M.; Fatih, M. Spermicidal activity of chelated complexes of bis(cyclopentadienyl)vanadium(IV). *Mol. Human Reprod*. **1998**, 4, 683–693.

[85] D'Cruz, O.J.; Donga, Y.; Uckun, F.M. Spermicidal Activity of Oxovanadium(IV) Complexes of 1,10-Phenanthroline, 2,2'-Bipyridyl, 5'-Bromo-2'-Hydroxyacetophenone and Derivatives in Humans. *Biol.Reprod.* **1999**, 60, 435-444.

[86] Wang, Z.; Bonner, J.C. Mechanism of extracellular signal-regulated kinase (ERK)-1 and ERK-2 activation by vanadium pentoxide in rat pulmonary myofibroblasts. *Am. J. Respir. Cell. Mol. Biol.* **2000**, 22, 590–596.

[87] Blazquez, C.; Galve-Roperh, I.; Guzmán, M. De novo-synthesized ceramide signals apoptosis in astrocytes via extracellular signal-regulated kinase. *FASEB J.* **2000**, 14, 2315–2322.

[88] Fu, Y.; Wang, Q.; Yang, X-G.; Yang, X-D.; Wang, K. Vanadyl bisacetylacetonate induced G1/S cell cycle arrest via high-intensity ERK phosphorylation in HepG2 cells. *J Biol. Inorg. Chem*. **2008**, 13, 1001–1009.

[89] D´Onofrio, F.; Le, M.Q.; Chiasson, J.L.; Srivastava, A.K. Activation of mitogen activated protein (MAP) kinases by vanadate is independent of insulin receptor autophosphorylation. *FEBS Lett.* **1994**, 340, 269–274.

[90] Okajima, T.; Nakamura, K.; Zhang, H.; Ling, N.; Tanabe, T.; Yasuda, T.; Rosenfeld, R.G. Sensitive colorimetric bioassays for insulin-like growth factor (IGF) stimulation of cell proliferation and glucose consumption: use in studies of IGF analogs *Endocrinology*. **1992**, 130, 2201-2212.

[91] Hissin, P.J.; Hilf, R. A fluorometric method for determination of oxidized and reduced glutathione in tissues. *Anal. Biochem*. **1976**, 74, 214-226.

[92] Bradford, M. A rapid and sensitive method for the quantitation of microgram quantities of protein utilizing the principle of protein-dye binding. *Anal. Biochem.* **1976**, 72, 249–254.

[93] Laemmli, U.K. Cleavage of structural proteins during the assembly of the head of bacteriophage T4. *Nature* **1970**, 227, 680–685.

[94] Shang, X.J.; Yao, G.; Ge, J.P.; Sun, Y.; Teng, W.H.; Huang, Y.F. Procyanidin Induces Apoptosis and Necrosis of Prostate Cancer Cell Line PC-3 in Mitochondrion-dependent Manner. *J. Androl.* **2009,** 30(2), 122-6.

Received: ????????????? Revised: ??????????????? Accepted: ?????????????